Rare Gas Measurements in 30 Stone Meteorites

P. Eberhardt, O. Eugster, J. Geiss, and K. Marti *

Physikalisches Institut, University of Berne, Switzerland

(Z. Naturforschg. **21 a**, 414—426 [1966]; received 30 November 1965)

The concentrations and isotopic composition of He, Ne and Ar in 29 chondrites and 1 achondrite have been determined. Detailed accounts of the experimental technique used and the reproducibility and accuracy obtained are given. The U,Th-He^4, and K-Ar ages derived from our results are in agreement with the already known age distributions of the different chondrite classes. Our measurements have revealed a linear correlation between the $(He^3/Ne^{21})_{spall}$ and the $(Ne^{22}/Ne^{21})_{spall}$ ratios, following the equation (constants for chondrites):

$$He^3/Ne^{21} = 2.40 + 23.4\,(Ne^{22}/Ne^{21} - 1)\ .$$

The significance of this correlation and its possible application in detecting diffusion losses are discussed. The radiation ages derived confirm the salient features observed in the radiation age distributions of the different chondrite classes. Five new meteorites with trapped gases were found (2 solar type, 3 planetary type).

1. General

During the last decade, the determination of the concentrations and isotopic compositions of rare gases in meteorites has become an important part of meteorite research and has given a great deal of information on the history of meteorites, the evolution of the solar system and on the intensity of cosmic radiation in the past. A considerable number of meteorites has been investigated and yet the accumulated body of data still seems to be insufficient to settle with statistical significance a number of important questions.

In this paper, we report and discuss concentrations and isotopic compositions of helium, neon and argon in 30 stone meteorites. In some of these meteorites, the isotopic abundances of krypton and xenon have also been determined [1].

It has been our aim in the present work to measure the three light rare gases with good relative and absolute accuracy in a restricted number of chondrites. The simultaneous determination of helium, neon and argon in the same sample is very important for the interpretation of the rare gas data. A high accuracy may reveal yet undiscovered correlations between different rare gas isotopes, radiation ages, radioactive ages, and other observational parameters. Very often results obtained in different laboratories have to be compared and thus a high absolute accuracy in the determination of isotopic compositions and concentrations is required.

Weathering and terrestrial temperatures may influence the rare gas content of a meteorite, and thus we have mainly investigated observed falls.

2. Meteorite Samples

The meteorite samples investigated were obtained from different collections and from some commercial sources. The relevant data on the meteorites (date of fall, recovered weight, fayalite content, classification, source of sample) are compiled in Table 1.

We were able to prove that two of our meteorite specimens are mislabelled. Magnetic measurements [8] showed that a meteorite specimen labelled Ausson and one labelled Mocs were both high iron chondrites. According to the classification in the literature [2, 3], however, both meteorites belong to the low iron class of chondrites. Such a variation of the chemical and mineralogical composition in one chondrite fall has never been observed yet and we must assume that some mislabelling has occurred.

We have a second specimen of Ausson indeed belonging to the low iron chondrite class. Its radiation age is lower by a factor of ten (to be publish-

* Present address: Department of Chemistry, University of California, La Jolla, Calif., U.S.A.

[1] K. Marti, P. Eberhardt, and J. Geiss, Z. Naturforschg. **21 a**, 398 [1966].

[2] G. T. Prior and M. H. Hey, Catalogue of Meteorites, British Museum, London 1953.

[3] B. Mason, Geochim. Cosmochim. Acta **27**, 1011 [1963].

Meteorite	Date of fall	Recovered weight kg	Fayalite content mol%	Classification	Source of sample
Atoka	9. 15. 1945	0.48	24	L	b
Baxter	1. 18. 1916	0.61	24	L	c
Benton	1. 16. 1949	5.4	31	LL	m
Bruderheim	3. 4. 1960	300	24	L	l
Calliham	found 1958	40	23	L	d
Colby (Wisconsin)	7. 4. 1917	105	25	L	c
Dhurmsala	7. 14. 1860	150	26	LL	e
Dimmitt	found	13.5	20	H	d
Finney	found	10.4	—	LL****	d
Harleton	5. 30. 1961	8.3	26	L	f
"H-Ausson"*	unknown	—	—	H	g
Kandahar (Afghanistan)	November 1959	0.68	24	L	h
Kesen	6. 12. 1850	135	17	H	c
Lanzenkirchen	8. 28. 1925	7	—	L	a
Marion, Kansas	found 1955	2.89	24	L	d
Maziba	9. 24 1942	5.0	25	L	b
Mezö-Madaras	9. 4. 1852	22.7	26	L	a
Mocs	2. 3. 1882	~300	24	L	i
Monte das Fortes	8. 23. 1950	4.9	24	L	j
Nerft	4. 12. 1864	10.25	23	L	a
Pribram	4. 7. 1959	9.5	20	H	k
"Pseudo-Pultusk"*	unknown	—	—	H	i
Saline	found***	31	18	H	c
St. Germain-du-Pinel	7. 4. 1890	~ 4	18	H	i
Shalka	11. 30. 1850	3.6**	—	D	a
Soko-Banja	10. 13. 1877	~80	27	LL	a
Tieschitz	7. 15. 1878	~28	—	L	a
Tysnes Island	5. 20. 1884	19.9	20	H	g
Waconda	found 1873	~50	25	L	a
Walters	7. 28. 1946	28	25	L	b

Table 1. Some relevant data on the investigated meteorites. Date of fall and recovered weight from PRIOR and HEY [2], MASON [3], KEIL [4], LEONARD [5]; fayalite content from MASON [3]. Classification: H=high iron chondrite; L=low iron chondrite; LL=amphoteric chondrite; D=diogenite (UREY and CRAIG [6], KEIL and FREDRIKSSON [7]). Sources of samples: [a] Prof. W. SCHOLLER, Naturhistorisches Museum, Wien; [b] Dr. E. P. HENDERSON, U.S. National Museum, Washington; [c] Prof. C. B. MOORE, Arizona State University, Tempe; [d] American Meteorite Laboratory, Denver; [e] Mineralien-Kontor Dr. F. KRANTZ, Bonn; [f] Prof. J. ARNOLD, University of California, San Diego; [g] Deyrolle, Paris; [h] Prof. M. GRÜNENFELDER, ETH, Zürich; [i] Mineralienhandlung Berger, Mödling; [j] Prof. A. DE CASTELLO BRANCO, Serviços Geologicos, Lisboa; [k] Prof. A. TUCEK, Narodni Museum, Praha; [l] Prof. R. E. FOLINSBEE, University of Alberta, Edmonton; [m] Proffs. R. DAVIES and O. SCHAEFFER, BNL, Brookhaven. * see text (chapter 2); ** probably much larger; *** possibly fell 11. 15. 1898; **** classification according to magnetic measurements (cf. EBERHARDT and GEISS [8]).

ed). The rare gas data of our high iron "Ausson" specimen are in good agreement with the results obtained by KIRSTEN, KRANKOWSKY, and ZÄHRINGER [9] on an alleged Ausson specimen. We thus conclude that the specimens measured by KIRSTEN et al. [9] and by us belong to the same, unknown high iron chondrite fall and we shall designate it as "H-Ausson".

The specimen labelled "Mocs" seems to belong to the Pultusk meteorite fall. The rare gas data are in fair agreement with results obtained on other specimens of Pultusk. Furthermore, meteorite specimens labelled Pultusk – obtained from the same commercial source as our alleged Mocs specimen – turned out to belong most likely to the Mocs meteorite fall [10]. It seems therefore that at

[4] K. KEIL, Fortschr. Mineral. **38**, 202 [1960].
[5] F. C. LEONARD, A Classificational Catalog of the Meteoritic Falls of the World, University of California press, Berkeley and Los Angeles 1956.
[6] H. C. UREY and H. CRAIG, Geochim. Cosmochim. Acta **4**, 36 [1953].
[7] K. KEIL and K. FREDRIKSSON, J. Geophys. Res. **69**, 3487 [1964].
[8] P. EBERHARDT and J. GEISS, in Isotopic and Cosmic Chemistry, dedicated to H. C. UREY (ed. H. CRAIG, S. L. MILLER, and G. J. WASSERBURG), North-Holland Publ. Co., Amsterdam 1964, p. 452.
[9] T. KIRSTEN, D. KRANKOWSKY, and J. ZÄHRINGER, Geochim. Cosmochim. Acta **27**, 13 [1963].
[10] H. HINTENBERGER, H. KÖNIG, L. SCHULTZ, and H. WÄNKE, Z. Naturforschg. **19 a**, 327 [1964], footnote 27.

some time specimens of Mocs and Pultusk have been confused and were subsequently sold with the wrong labelling. Therefore, we will designate our sample as "Pseudo-Pultusk".

3. Experimental Technique

3.1 Sample Preparation

For the analysis a piece of 2 to 5 gms of the meteorite specimen was chosen, if possible far away from any fusion crust. No samples were used which had been powdered previously. Any remaining fusion crust and surface contaminations were removed with a small dry abrasive wheel. A new wheel was used for each sample. The cleaned specimen was crushed on a stainless steel plate to a grain size finer than approximately 1 mm. Care was taken not to pulverize the sample too finely. Aliquots of 0.1 to 1 gram were then used for the individual rare gas determinations.

3.2 Rare Gas Extraction and Purification

Fig. 1 is a schematic drawing of the rare gas extraction and purification system used in this work. The meteorite samples were weighed into small Al-containers. Up to nine meteorite samples could be extracted without braking the vacuum. The whole extraction system was baked at 270 °C prior to extraction. The molybdenum crucible and the extraction jacket were thoroughly pre-degassed. The samples were heated to 70 °C for several hours to remove adsorbed atmospheric gases. The rare gases were extracted by melting the meteorite samples at 1700–1800 °C for 30 minutes. The evolved gases were purified in two steps with Ti-sponge and Ti-foil and subsequently Ar and He–Ne were transferred into separate sample tubes. Supremax glass sample tubes were used for the He–Ne fraction. All samples were subjected to an additional cleaning with hot Ti-foil, a hot CuO–Pd-mixture and hot CuO on the sample inlet system of the mass spectrometers.

In each set of samples at least one aliquot of the meteorites Dhurmsala or Kandahar was included. The completeness of the extraction was tested by at least one re-extraction at higher crucible temperature. The extraction blanks of our procedure were determined from extractions of empty aluminum containers, small meteorite samples of relatively low neon content, and from re-extractions. Blanks for He, Ne and Ar were 12, 0.2 and 0.5×10^{-8} cc STP respectively. For some samples measured early in this investigation, the neon and argon blanks were somewhat higher.

At least three extractions on aliquots of each meteorite sample were performed, two without spike for measuring the isotopic composition and one with a He^3–Ne^{22}–Ar^{38} spike for determining the concentrations by the isotopic dilution method. The sample sizes of the two extractions without spike were varied by about a factor of two. As a check, we have also calculated concentrations from ion beam intensities in all runs. The figures obtained in this way agree with the isotopic dilution results within 10%.

3.3 Mass Spectrometry

The rare gas samples were analyzed on all-glass, sector type, 60 degree, 10 cm radius of curvature, statically operated, UHV mass spectrometers with direct ion collection (without multiplier). No source magnet was employed for the helium and neon measurements. The sensitivity used was in the range of 2×10^{-6}, 4×10^{-6} and 3×10^{-5} amperes/cc STP for helium, neon and argon respectively. For most measurements, corrections due to machine background corresponded to less than 0.02×10^{-8} cc STP He^3 on mass 3 (HD), to less than 0.05×10^{-8} cc STP Ne^{20} on mass 20 (Ar^{++}) and to less than 0.1×10^{-8} cc STP Ne^{22} on mass 22 (CO_2^{++}). The mass spectrometer blank of atmospheric helium, neon and argon was always less than 10% of the extraction blank. Two spectrometers were employed in order to minimize the memory effect from the enriched gases used as spike. Mass discriminations in the spectrometer were always small (less than 1.5 percent per mass unit) and, furthermore, were always determined and corrected by measuring atmospheric argon and neon standards and a He^3/He^4 mixture prepared from calibrated amounts of pure He^3 and He^4. All our measurements are based on the ratios $Ar^{40}/Ar^{36} = 295.5$ (Nier [11]) and $Ne^{20}/Ne^{22} = 9.80$ (Eberhardt, Eugster, and Marti [12]) for atmospheric argon and neon.

3.4 Reproducibility and Accuracy

As mentioned above, a sample of a standard meteorite (Dhurmsala or Kandahar) was included in each set of meteorite samples. We have thus accumulated a considerable number of analyses of these two meteorites and the overall reproducibility of our whole measuring procedure can be calculated from these data. Tables 2 and 3 give the standard deviations for these repeated analyses, along with the average deviations observed between the duplicate analyses performed on all the other meteorites.

The observed standard deviations, and thus the errors for our experimental rare gas determination technique, are all smaller than 4% (except the Ar isotopes for Dhurmsala, see below). The Ne^{22}/Ne^{21} ratio has a standard deviation of less than one percent. The Ar^{40}/Ar^{36} and – to a lesser degree – the Ar^{40}/Ar^{38} ratios of Dhurmsala have a much higher standard deviation than those of Kandahar and of all the other samples. However, the Ar^{40}/Ar^{38}_{spall} ratio and also the absolute amount of Ar^{40} in Dhurmsala have standard deviations comparable to those obtained for the other meteorites. The large variations of Ar^{40}/Ar^{36}

[11] A. O. Nier, Phys. Rev. **77**, 789 [1950].

[12] P. Eberhardt, O. Eugster, and K. Marti, Z. Naturforschg. **20 a**, 623 [1965].

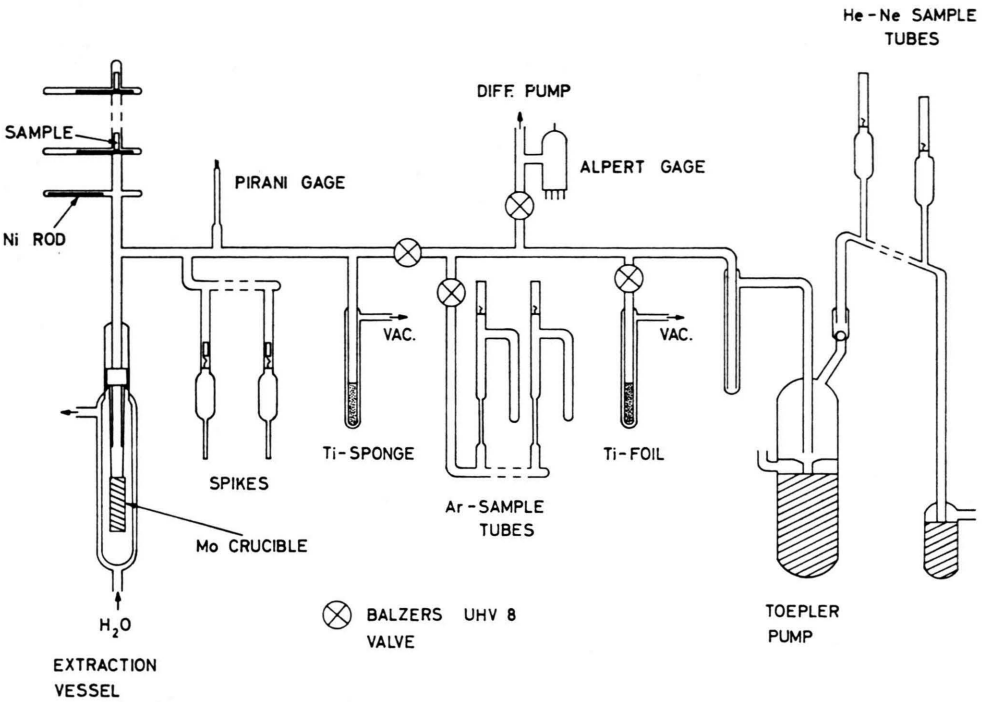

Fig. 1. Diagram of rare gas extraction and purification system used in this work.

meteorite	number of analyses	$\frac{He^3}{He^4}$	$\frac{Ne^{20}}{Ne^{21}}$	$\frac{Ne^{22}}{Ne^{21}}$	$\frac{Ar^{40}}{Ar^{36}}$	$\frac{Ar^{40}}{Ar^{38}}$	$\frac{Ar^{40}}{Ar^{38}_{spall}}$
Dhurmsala	12	1.8%	3.7%	0.8%	28 %*	11 %*	5.7%
Kandahar	9	2.7%	3.2%	0.8%	3.8%	3.5%	4.3%
Other samples		2.0%	4.0%	0.9%	2.4%	2.2%	3.3%

Table 2. Standard deviations of individual isotopic ratio measurements as derived from repeated analyses of aliquots of the Dhurmsala and Kandahar chondrites (sample sizes 0.3—0.7 gm). No measurements were discarded. Also given are the average deviations observed between the duplicate analyses of all the other meteorites. * The large variations in these isotopic ratios are presumably due to fluctuations in the trapped gas content (see text).

and Ar^{40}/Ar^{38} observed in different aliquots of Dhurmsala are thus probably due to fluctuations in the trapped gas content of this meteorite.

meteorite	number of analyses	He^4	Ne^{21}	Ar^{40}
Dhurmsala	4	0.6%	3.5%	1.5%
Kandahar	3	1.6%	1.2%	0.8%

Table 3. Standard deviations of individual isotopic concentration measurements by isotopic dilution as derived from repeated analyses of aliquots of the Dhurmsala and Kandahar chondrites (samples sizes 0.3—0.7 gm). No measurements were discarded.

Standards with known amounts of pure helium, neon and argon were prepared by filling calibrated sample tubes with a known gas pressure. Two independent methods were used for obtaining and measuring the pressure: (1) beginning with a high pressure measured with a mercury U-tube manometer, the gas was expanded into known volumes until the pressure was sufficiently low; (2) the filling pressure was directly measured with a McLeod gauge. The spikes were subsequently calibrated against these standards. The agreement finally obtained was better than 2%.

4. Results

The results of our rare gas measurements are compiled in Table 4. The chondrites are classified according to Urey and Craig [6] into high iron chondrites (H-chondrites), low iron chondrites (L-chondrites) and amphoteric chondrites (LL-chondrites [7]). Eberhardt and Geiss [8] have shown that such a classification is indeed justified for the discussion of the rare gas data of chondrites and that significant

Meteorite	He^3	He^4	Ne^{20}	Ne^{21}	Ne^{22}	Ar^{36}	Ar^{38}	Ar^{40}	$\frac{He^4}{He^3}$	$\frac{Ne^{20}}{Ne^{21}}$	$\frac{Ne^{22}}{Ne^{21}}$	$\frac{Ar^{40}}{Ar^{36}}$	$\frac{Ar^{36}}{Ar^{38}}$
L-Chondrites													
Atoka	7.6	570	1.11	1.23	1.38	0.83	0.33	6080	75.1	0.90	1.120	7350	2.5
	±0.4	±20	±0.09	±0.06	±0.08	±0.04	±0.05	±200	±2.0	±0.05	±0.030	±250	±0.4
Baxter	36.6	490	6.25	6.65	7.75	1.23	1.18	3380	13.4	0.94	1.165	2750	1.04
	±1.5	±13	±0.30	±0.25	±0.30	±0.05	±0.06	70	±0.3	±0.03	±0.015	± 90	±0.03
Bruderheim	52.4	561	8.8	9.90	10.9	1.56	1.56	1155	10.7	0.89	1.100	742	1.00
	±2.5	±20	±0.7	±0.50	±0.116	±0.09	±0.14	± 45	±0.3	±0.05	±0.020	± 20	±0.07
Calliham	44.6	321	8.8	9.70	10.6	1.49	1.16	330	7.2	0.91	1.090	222	1.28
	±3.0	± 9	±0.5	±0.35	±0.4	±0.06	±0.06	± 7	±0.4	±0.03	±0.010	± 7	±0.04
Colby,	45.0	563	9.7	10.6	11.5	1.89	1.50	2950	12.5	0.92	1.080	1560	1.26
Wisconsin	±2.0	±15	±0.5	±0.4	±0.5	±0.07	±0.07	± 60	± 0.3	±0.03	±0.010	± 50	±0.04
Harleton	70.4	602	11.7	12.7	14.2	2.15	1.92	970	8.55	0.92	1.120	450	1.12
	±3.0	±20	±0.8	±0.6	±0.8	±0.12	±0.14	± 35	±0.17	±0.04	±0.020	± 20	±0.05
Kandahar	40.5	1055	7.8	9.00	9.80	1.51	1.28	5790	26.1	0.87	1.090	3840	1.18
	±1.2	±20	±0.3	±0.25	±0.30	±0.04	±0.04	± 90	±0.4	±0.02	±0.010	± 80	±0.02
Lanzen-	66.8	488	14.5	15.9	17.6	3.12	2.48	1285	7.3	0.92	1.105	415	1.26
kirchen	±3.5	±13	±0.7	±0.6	±0.7	±0.35	±0.30	± 25	±0.3	±0.03	±0.010	± 30	±0.04
Marion,	64.0	1505	12.3	13.4	14.8	7.40	2.60	7760	23.5	0.92	1.105	1050	2.84
Kansas	±2.5	±40	±0.6	±0.5	±0.6	±0.40	±0.18	±150	±0.5	±0.03	±0.010	± 50	±0.12
Maziba	46.9	1225	5.7	6.25	7.55	1.25	1.10	5900	26.1	0.91	1.210	4720	1.14
	±2.0	±45	±0.4	±0.30	±0.45	±0.06	±0.07	±200	±0.6	±0.04	±0.020	±150	±0.09
Mezö-	51.3	836	11.8	11.1	12.5	52.2	11.3	1255	16.3	1.06	1.125	24.0	4.61
Madaras	±2.5	±25	±0.6	±0.4	±0.5	±2.5	±0.6	± 25	±0.5	±0.04	±0.010	± 1.0	±0.10
Mocs	24.5	707	5.5	6.65	7.00	1.31	0.92	5630	28.1	0.83	1.055	4300	1.43
	±1.0	±18	±0.5	±0.25	±0.25	±0.06	±0.05	±120	±0.6	±0.06	±0.010	±170	±0.04
Monte das	51.2	1425	10.7	11.6	12.8	1.92	1.59	5620	27.8	0.92	1.100	2920	1.21
Fortes	±2.0	±40	±0.6	±0.4	±0.5	±0.20	±0.20	±120	±0.6	±0.03	±0.010	±300	±0.10
Nerft	63.5	470	12.0	13.0	14.0	2.02	1.98	270	7.4	0.92	1.080	133.2	1.02
	±2.5	±12	±0.6	±0.5	±0.5	±0.08	±0.10	± 6	±0.2	±0.03	±0.010	± 4.0	±0.03
Tieschitz	45.8	1685	9.0	7.50	9.15	22.8	5.34	2280	36.8	1.20	1.220	100	4.27
	±1.5	±45	±0.5	±0.25	±0.35	±0.9	±0.25	± 50	±0.7	±0.05	±0.010	± 3	±0.10
Waconda	24.7	1305	5.5	5.90	6.43	1.24	0.92	5620	52.9	0.93	1.090	4530	1.35
	±1.0	±35	±0.3	±0.20	±0.25	±0.05	±0.05	±120	±1.1	±0.03	±0.010	±150	±0.04
Walters	4.4	331	1.16	1.27	1.33	0.98	0.33	2140	74.7	0.91	1.050	2180	2.94
	±0.2	±15	±0.09	±0.06	±0.08	±0.05	±0.04	± 70	±2.5	±0.05	±0.030	± 70	±0.30
H-Chondrites													
Dimmitt	3.8	4030	58.2	1.83	6.74	7.50	1.58	1950	1075	31.8	3.68	259	4.76
	±0.2	±100	±3.0	±0.07	±0.30	±0.30	±0.07	± 40	±30	±1.0	±0.07	± 8	±0.12
"H-Ausson"	101	1610	19.5	21.7	23.9	3.53	3.36	6110	15.9	0.90	1.100	1730	1.05
	±4	±40	±1.0	±0.8	±0.9	±0.13	±0.17	±130	± 0.3	±0.03	±0.010	± 50	±0.03
Kesen	12.2	1455	1.90	2.62	2.82	1.95	0.67	5300	119	0.72	1.075	2720	2.89
	±0.5	±40	±0.28	±0.09	±0.11	±0.07	±0.03	±110	± 3	±0.10	±0.020	± 90	±0.09
"Pseudo-	8.9	5690	16.2	2.02	3.35	2.35	0.65	5710	639	8.0	1.66	2430	3.59
Pultusk"	±0.4	±150	±0.9	±0.07	±0.15	±0.09	±0.03	±120	±15	±0.3	±0.03	± 80	±0.10
Pribram	23.9	1315	5.0	5.10	5.56	1.10	0.77	4170	55.0	0.98	1.090	3800	1.43
	±1.2	± 50	±0.4	±0.25	±0.30	±0.06	±0.09	±140	± 1.6	±0.04	±0.020	±120	±0.14

Table 4

Meteorite	He^3	He^4	Ne^{20}	Ne^{21}	Ne^{22}	Ar^{36}	Ar^{38}	Ar^{40}	$\frac{He^4}{He^3}$	$\frac{Ne^{20}}{Ne^{21}}$	$\frac{Ne^{22}}{Ne^{21}}$	$\frac{Ar^{40}}{Ar^{36}}$	$\frac{Ar^{36}}{Ar^{38}}$
Saline	9.4	1245	1.56	1.79	2.01	1.91	0.64	4390	132	0.87	1.125	2290	3.00
	±0.4	±35	±0.09	±0.07	±0.08	±0.07	±0.03	±90	±3	±0.04	±0.015	±70	±0.10
St. Germain-du-Pinel	9.5	1260	2.08	2.54	2.69	1.46	0.59	5150	132	0.82	1.060	3520	2.48
	±0.4	±35	±0.15	±0.09	±0.11	±0.06	±0.03	±110	±4	±0.05	±0.015	±110	±0.07
Tysnes Island	38.4	109000	415	3.22	38.6	25.5	5.25	4820	2840	129	12.0	189	4.86
	±1.5	±3000	±25	±0.15	±2.0	±2.7	±0.60	±100	±70	±3	±0.2	±18	±0.15
LL-Chondrites													
Benton	47.5	1335	8.6	9.75	10.7	1.18	1.37	5370	28.1	0.88	1.100	4540	0.86
	±2.0	±35	±0.45	±0.35	±0.4	±0.05	±0.07	±110	±0.6	±0.03	±0.010	±140	±0.02
Dhurmsala	14.0	529	3.77	4.05	4.35	1.16	0.64	3410	37.8	0.93	1.075	2940	1.80
	±0.4	±11	±0.13	±0.12	±0.14	±0.12	±0.08	±60	±0.5	±0.02	±0.010	±300	±0.10
Finney	29.4	708	3.80	3.92	4.65	1.13	0.68	4100	24.1	0.97	1.185	3620	1.67
	±1.2	±18	±0.20	±0.14	±0.17	±0.04	±0.03	±90	±0.6	±0.03	±0.010	±110	±0.05
Soko Banja	110	1750	24.3	26.7	29.5	6.78	4.16	9490	15.9	0.91	1.105	1400	1.63
	±4	±45	±1.2	±0.9	±1.1	±0.25	±0.20	±200	±0.4	±0.03	±0.010	±50	±0.05
Diogenite													
Shalka	39.4	209	5.9	6.20	7.20	0.57	0.28	120	5.3	0.94	1.160	211	2.0
	±2.0	±4	±0.3	±0.20	±0.30	±0.12	±0.13	±5	±0.2	±0.03	±0.020	±40	±0.8

Table 4. Results of rare gas analyses. All concentrations in units of 10^{-8} cc STP/gm.

differences exist between the age distributions of L- and H-chondrites.

The reproducibility of our experimental procedure, as determined from the repeated analyses of Dhurmsala and Kandahar (see 3.4), has served as basis for the assignment of errors. Additional factors, such as sample size or absolute rare gas concentration, were also taken into account. The absolute error of our gas standards used for spike calibrations is included in the errors given for the concentrations.

With a few exceptions, we had chosen meteorites for which no or only incomplete rare gas data were available in the literature at the time of measurement. In the meantime, however, rare gas results have been published of an additional number of meteorites included in our investigation. A comparison between our results and those published by other investigators is hampered by the following two factors:

a) The meteorite samples used are not aliquots and thus some variations in the rare gas contents between different samples cannot be excluded. However, the uranium, thorium and potassium contents in ordinary chondrites are fairly constant [9, 13–20], and thus radiogenic He^4 and Ar^{40} are not expected to vary for different samples of the same meteorite, provided each sample represents a good average. If very small samples are used, variations may be introduced by mineralogical and chemical inhomogeneities. Large variations in the trapped gas content in the same meteorite do occur, and therefore no comparison of this gas component is possible. Of course, also the possibility exists that meteorite samples are mislabelled.

b) No individual errors are assigned to most of the published data.

The average relative deviations $|\bar{\delta}|$ and the mean of the relative deviations $\bar{\delta}$ observed between the

[13] H. Hamaguchi, G. W. Reed, and A. Turkevich, Geochim. Cosmochim. Acta **12**, 337 [1957].
[14] G. L. Bate, J. R. Huizenga, and H. A. Potratz, Geochim. Cosmochim. Acta **16**, 88 [1959].
[15] H. König and H. Wänke, Z. Naturforschg. **14 a**, 866 [1959].
[16] G. W. Reed, K. Kigoshi, and A. Turkevich, Geochim. Cosmochim. Acta **20**, 122 [1960].
[17] G. G. Goles and E. Anders, Geochim. Cosmochim. Acta **26**, 723 [1962].
[18] G. Edwards and H. C. Urey, Geochim. Cosmochim. Acta **7**, 154 [1955].
[19] G. Edwards, Geochim. Cosmochim. Acta **8**, 285 [1955].
[20] J. Geiss and D. C. Hess, Astrophys. J. **127**, 224 [1958].

published and our results are given in Table 5. The average relative deviations are two to eight times larger than the accuracy of our own results. The best agreement is obtained for the Ne^{22}/Ne^{21} ratio. This is not surprising because this ratio varies by only 20% between different meteorites, whereas all the other ratios are much less constant. The mean of the relative deviations is, with the exception of the Ne^{20}/Ne^{21} ratio, always much smaller than the average deviation. Thus, no large systematic differences between our results and the published data seem to occur. The discrepancy in the Ne^{20}/Ne^{21} ratio may be due to an underestimation of the Ne^{20} blank correction in many of the literature data, and to the use of the old value $Ne^{20}/Ne^{22} = 10.3$ for terrestrial neon. This should also lead to systematic differences in the Ne^{22}/Ne^{21} values.

It is important to consider these random differences which seem to exist between rare gas measurements performed by different laboratories, if conclusions are based on results from many investigators. As an illustration, let us consider a set of meteorites created in one break-up process. They will have exactly the same radiation age. If these meteorites were measured by different laboratories, a minimum line width of 20% for the radiation age distribution would result from the experimental errors. If the radiation ages are derived from the concentration of He^3 alone, an additional line broadening by approximately 30% would occur, due to variations in shielding. Thus, the measuring and evaluation technique used transforms this initial δ-function into a broad peak with a line width of approximately 40%. If Ne^{21} is used instead of He^3 the resulting line broadening would be even larger (cf. chapter 6.2). Thus, individual events in the history of meteorite parent bodies will be masked if they occur too frequently.

5. Radiogenic Ages

The potassium content of most L- and H-chondrites is constant within $\pm 10\%$ [9, 18–20] and also uranium and thorium do not show large variations [13–17]. It is therefore possible to calculate K^{40}-Ar^{40} and U, Th-He^4 ages from the rare gas data alone (Table 6). Average uranium, thorium and potassium contents of 0.012, 0.043 and 850 ppm respectively were used for L- and H-chondrites. He^4 was corrected for the contribution from spallation assuming $He^4/He^3 = 4$ in spallation produced helium [9]. This correction is small except for some meteorites with U,Th-He^4 ages below 10^9 years. The following decay constants were used for the calculation of the ages:

$$\lambda(U^{238}) = 1.54 \times 10^{-10} \text{ yrs}^{-1};$$
$$\lambda(U^{235}) = 9.8 \times 10^{-10} \text{ yrs}^{-1};$$
$$\lambda(Th^{232}) = 4.99 \times 10^{-11} \text{ yrs}^{-1};$$
$$\lambda_{tot}(K^{40}) = 5.46 \times 10^{-10} \text{ yrs}^{-1};$$
$$\lambda_k(K^{40}) = 6.02 \times 10^{-11} \text{ yrs}^{-1}.$$

The potassium content of LL-chondrites is not as constant as in L- and H-chondrites (KAISER and ZÄHRINGER [21]). Thus, no radiogenic ages are given for this chondrite class.

The U,Th-He^4 and K-Ar^{40} ages obtained for the investigated chondrites show the general behavior characteristic for chondrites:

1. Most K-Ar^{40} ages of chondrites lie between 3.5 and 4.6×10^9 years (GEISS and HESS [20]; KIRSTEN, KRANKOWSKY, and ZÄHRINGER [9]).

	He^3	He^4	Ne^{20}	Ne^{21}	Ne^{22}	Ar^{36}	Ar^{38}	Ar^{40}	$\frac{He^4}{He^3}$	$\frac{Ne^{20}}{Ne^{21}}$	$\frac{Ne^{22}}{Ne^{21}}$	$\frac{Ar^{40}}{Ar^{36}}$	$\frac{Ar^{36}}{Ar^{38}}$
Average relative deviation $\overline{\lvert\delta\rvert}$	8%	14%	11%	10%	12%	16%	17%	9%	12%	9%	4%	12%	10%
Mean of relative deviations $\bar{\delta}$	+4%	−1%	+4%	−3%	−6%	−9%	−8%	−5%	+6%	+8%	−2%	−6%	+1%
Number of comparisons	24	22	18	21	20	10	11	12	21	17	20	10	11

Table 5. Average relative deviations $\overline{|\delta|} = \frac{1}{n} \sum \left| \left(\frac{x_i}{x_0} - 1 \right) \right|$ and mean of relative deviations $\bar{\delta} = \frac{1}{n} \sum \left(\frac{x_i}{x_0} - 1 \right)$ observed between our results and those of other workers. x_0: our measurements, x_i: published measurements. Values deviating by more than 50% from our own results have been discarded, as well as those meteorites containing trapped gases. $\bar{\delta}$ is a measure for systematic differences between the published and our results, $\overline{|\delta|}$ indicates random fluctuations.

[21] W. KAISER and J. ZÄHRINGER, Z. Naturforschg. **20 a**, 963 [1965].

Sample	He^3_{spall}	Ne^{21}_{spall}	Ar^{38}_{spall}	$\frac{He^3_{spall}}{Ne^{21}_{spall}}$	$\frac{Ne^{22}_{spall}}{Ne^{21}_{spall}}$	He^3-age	U,Th-He^4 age	K-Ar-age
	10^{-8} cc STP/gm					10^6 years		
L-Chondrites								
Atoka	7.6	1.23	0.21	6.18	1.120	3.8	1800	4440
Baxter	36.5	6.65	1.08	5.49	1.160	18.2	1200	3470
Bruderheim	52.4	9.9	1.44	5.29	1.100	26.2	1200	1950
Calliham	44.6	9.7	1.00	4.60	1.090	22.3	520	780
Colby, Wisconsin	45.0	10.6	1.31	4.25	1.080	22.5	1300	3250
Harleton	70.4	12.7	1.73	5.54	1.12	35.2	1100	1730
Kandahar	40.5	9.0	1.14	4.50	1.090	20.2	2700	4350
Lanzenkirchen	66.8	15.9	2.16	4.20	1.105	33.4	780	2080
Marion, Kansas	64.0	13.4	1.39	4.78	1.105	32.0	3450	4860
Maziba	46.9	6.25	0.99	7.50	1.210	23.4	3000	4390
Mezö-Madaras	51.3	11.1	—	4.62	1.110	25.6	2050	2050
Mocs	24.5	6.65	0.77	3.68	1.060	12.2	1950	4310
Monte das Fortes	51.2	11.6	1.40	4.41	1.100	25.6	3400	4300
Nerft	63.5	13.0	1.82	4.88	1.080	31.8	760	660
Tieschitz	45.8	7.5	—	6.11	1.195	22.9	—	2860
Waconda	24.7	5.9	0.78	4.19	1.085	12.4	3350	4300
Walters	4.4	1.27	0.17	3.46	1.050	2.2	1100	2770
H-Chondrites								
Dimmitt	3	1.67	—	—	—	1.5	—	2640
"H-Ausson"	101	21.7	3.1	4.65	1.100	50.5	3350	4440
Kesen	12.2	2.62	0.35	4.66	1.090	6.1	3700	4200
"Pseudo-Pultusk"	7.7	1.98	0.24	—	—	3.8	—	4330
Pribram	23.9	5.1	0.64	4.69	1.085	12.0	3400	3810
Saline	9.4	1.79	0.32	5.25	1.125	4.7	3350	3890
St. Germain-du-Pinel	9.5	2.54	0.36	3.74	1.065	4.8	3400	4150
Tysnes Island	—	2.0	—	—	—	(4)	—	4040
LL-Chondrites								
Benton	47.5	9.75	1.31	4.87	1.100	23.8	—	—
Dhurmsala	14.0	4.05	0.48	3.46	1.070	7.0	—	—
Finney	29.4	3.92	0.53	7.50	1.180	14.7	—	—
Soko Banja	110	26.7	3.3	4.12	1.105	55	—	—
Diogenite								
Shalka	39.4	6.20	0.20	6.35	1.155	—	—	—

Table 6. Concentrations and ratios of spallation produced isotopes, radiation ages and radiogenic ages of investigated meteorites.

2. U,Th-He^4 ages are either concordant or lower than K-Ar^{40} ages, in the latter case indicating diffusion loss (EBERHARDT and HESS [22]; ANDERS [23]).
3. The age distribution of L- and H-chondrites is different, implying different histories (EBERHARDT and GEISS [8]; KEIL [24]; ANDERS [25]).

All these features can be easily deduced from a histogram of the K-Ar^{40} ages, as given in Fig. 2. In addition to our results also all other known chondrite ages have been plotted (cf. ZÄHRINGER [26]). However, only meteorites with concordant He^4 and Ar^{40} ages have been included. We define these two ages as concordant, if the He^4 age does not deviate by more than 25% from the Ar^{40} age. This rather generous definition of concordance has to be used because of the uncertainty in the uranium, thorium and potassium contents, and also in view of the experimental errors of the rare gas concentrations. Concordant ages are much more frequent for the H-chondrites than for the L-chondrites [26] (75% against 42%). Several explanations for this systematic difference between the two chondrite classes seem possible: (1) The minerals in L-chondrites have larger diffusion coefficients for rare gases than those in H-chondrites. (2) The grain size distributions are different. (3) The temperature in L-chondrites was on the average higher than that in H-chondrites. (4) The L-chondrites have been reheated at some time in their history, resulting in

[22] P. EBERHARDT and D. C. HESS, Astrophys. J. **131**, 38 [1960].
[23] E. ANDERS, Rev. Mod. Phys. **34**, 287 [1962].
[24] K. KEIL, Nature **203**, 511 [1964].
[25] E. ANDERS, Space Sci. Rev. **3**, 583 [1964].
[26] J. ZÄHRINGER, Chronology of Chondrites with Rare Gas Isotopes, preprint [1965].

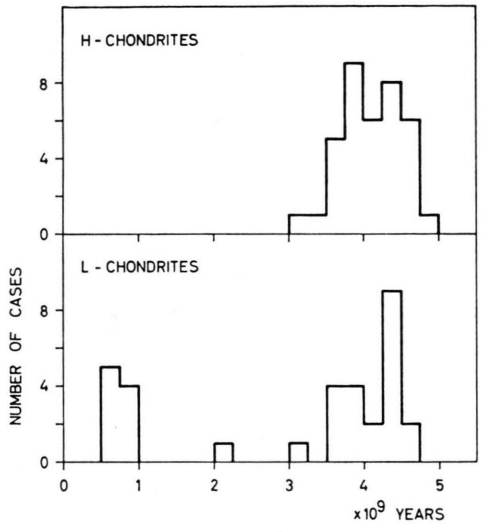

Fig. 2. Histogram of K/Ar^{40} ages. Only meteorites with concordant ages (He^4 age within $\pm 25\%$ of the $K\text{-}Ar^{40}$ age) are included. Ages from this paper and from summary in ZÄHRINGER's [26] publication.

total or partial loss of the rare gases. The occurrence of a sizable number of L-chondrites with concordant ages of around 600 m.y. makes the last of the four explanations the most likely one (ANDERS [25]).

6. Spallation Produced Isotopes

In Table 6 the concentrations of spallation produced He^3, Ne^{21}, and Ar^{38} of the investigated meteorites are listed. A correction for trapped gases (primordial gases) was applied, using the ratios $He^4/He^3 = 3500$; $Ne^{20}/Ne^{21} = 340$; $Ne^{20}/Ne^{22} = 11.4$ and $Ar^{36}/Ar^{38} = 5.35$ in the trapped component; $Ne^{20}/Ne^{21} = 0.9$ and $Ar^{36}/Ar^{38} = 0.65$ in the spallation component. Ar^{40} was not corrected.

With the exception of the three gas-rich meteorites, Tysnes Island, "Pseudo-Pultusk" and Dimmitt, the corrections for He^3 and Ne^{21} were less than 0.1% and for Ne^{22} less than 2%. Thus, they cannot introduce an appreciable error, even if the above assumed isotopic compositions of the trapped component should show some variations from one meteorite to the other. In most cases the correction for trapped Ar^{38} was less than 40%.

6.1 Correlation Between Spallation Produced Isotopes

It has been recognized for some time that certain correlations exist between spallation produced isotopes in iron meteorites [27, 28]. These correlations are in agreement with general spallation theory [29, 30]. From the abundance ratio of spallation produced isotopes such as Ar^{38} and Ne^{21} the hardness of the irradiation spectrum in the meteorite sample itself can be calculated [29], and thus the amount of shielding and the pre-atmospheric mass of an iron meteorite can be estimated [31].

The first measurements of rare gases in stone meteorites showed that in most chondritic meteorites the ratio of spallation produced isotopes are fairly constant. Large variations did, of course, occur between chondrites and the different classes of achondrites [20, 22, 32–34]. In the last few years, it was then recognized that the He^3/Ne^{21} ratio in chondrites is not constant and in extreme cases variations by a factor of three or more have been observed [9, 35]. As this effect could not be explained by differences in chemical composition, it was thought that it is due to variations in shielding [9] and to preferential diffusion loss of He^3.

HINTENBERGER, VILCSEK, and WÄNKE [36] have shown that certain minerals in the chondrite Breitscheid have indeed lost He^3, indicating that diffusion has affected the He^3/Ne^{21} ratio of 3.8. It is reported [37] that the low He^3/Ne^{21} ratios of 1.42 and 0.67 for Cullison and Seres respectively are also due to diffusion.

However, Parnallee with $He^3/Ne^{21} = 2.73$ does not seem to have suffered diffusion losses [37]. Thus, the observed variations in the He^3/Ne^{21} ratio cannot be explained by diffusion loss alone.

[27] K. H. EBERT and H. WÄNKE, Z. Naturforschg. **12a**, 766 [1957].
[28] P. SIGNER and A. O. NIER, J. Geophys. Res. **65**, 2947 [1960].
[29] J. GEISS, H. OESCHGER, and U. SCHWARZ, Space Sci. Rev. **1**, 197 [1962].
[30] J. R. ARNOLD, M. HONDA, and D. LAL, J. Geophys. Res. **66**, 3519 [1961].
[31] P. SIGNER and A. O. NIER, in Researches in Meteorites (ed. C. B. MOORE), John Wiley & Sons, New York 1962.
[32] A. EBERHARDT and P. EBERHARDT, Helv. Phys. Acta **33**, 593 [1960] and Z. Naturforschg. **16a**, 236 [1961].
[33] H. STAUFFER, J. Geophys. Res. **66**, 1513 [1961].
[34] H. STAUFFER, J. Geophys. Res. **67**, 2023 [1962].
[35] H. HINTENBERGER, H. KÖNIG, L. SCHULTZ, and H. WÄNKE, Z. Naturforschg. **19a**, 327 [1964].
[36] H. HINTENBERGER, E. VILCSEK, and H. WÄNKE, Z. Naturforschg. **19a**, 219 [1964].
[37] H. HINTENBERGER, H. KÖNIG, L. SCHULTZ, and H. WÄNKE, Z. Naturforschg. **20a**, 983 [1965].

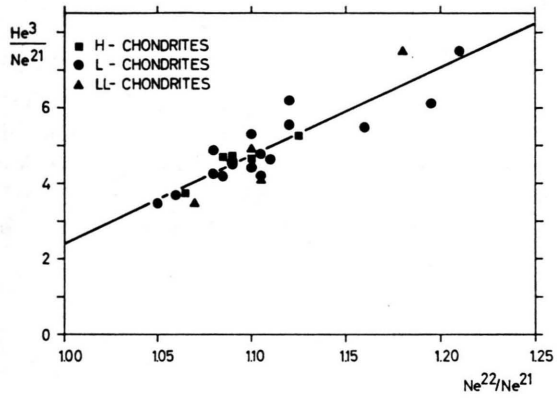

Fig. 3. $(He^3/Ne^{21})_{spall}$ versus $(Ne^{22}/Ne^{21})_{spall}$ diagram for chondrites. Data from this paper only. The correlation line has been calculated by the least square method.

From our results, as given in Table 6, we have found that a strong correlation exists between the $(He^3/Ne^{21})_{spall}$ and $(Ne^{22}/Ne^{21})_{spall}$ ratios. Fig. 3 shows this correlation in a $He^3/Ne^{21} - Ne^{22}/Ne^{21}$ diagram. Only our measurements have been included. The correlation seems to be linear within the errors of our measurements and the straight line drawn in Fig. 3 has been calculated by the least square method. It is represented by the equation

$$He^3/Ne^{21} = C + m\left(\frac{Ne^{22}}{Ne^{21}} - 1\right) \qquad (1)$$

with $C = 2.40$ and $m = 23.4$.

Among the published rare gas data on chondrites, only those of KIRSTEN, KRANKOWSKY, and ZÄHRINGER [9] show this correlation, but with a somewhat larger scatter than our measurements. The correlation is not clearly visible in the results of other authors, except for meteorites with extreme He^3/Ne^{21} ratios.

Three parameters can influence the position of a meteorite in the $He^3/Ne^{21} - Ne^{22}/Ne^{21}$ diagram: a) chemical composition; b) cosmic ray energy spectrum; c) diffusion loss.

6.1.1 Chemical Composition

In stone meteorites the neon isotopes are produced almost exclusively from spallation reactions on the elements sodium to sulphur. In chondrites magnesium alone contributes about 2/3 of the total production, and silicon a large fraction of the remainder [34, 38]. The He^3 production rate is similar for all elements.

The average MgO content of the three classes of chondrites differs slightly. L-chondrites contain on the average 6% and LL-chondrites 8% more MgO than H-chondrites [6, 39]. The average variation of the MgO content within one of these chondritic classes is about ±2% (CRAIG [39]). The variations of SiO_2 go roughly parallel with those of MgO, and therefore the ratio MgO/SiO_2 is quite constant. Thus, differences in the chemical composition between the chondrites will not influence the Ne^{22}/Ne^{21} ratio and can only lead to variations of ±5% in the He^3/Ne^{21} ratio.

The systematic differences in the MgO contents between the three chondrite classes should result in slightly different correlation lines. The slope m and the constant C in Eq. (1) should differ by approximately 6% between H and L and by 8% between H- and LL-chondrites. However, with the present-day accuracy and the rather limited number of measurements, these differences are masked by experimental error, and it is justified to treat all chondrites as one class.

6.1.2 Cosmic Ray Energy and Composition Spectrum

The production ratio of two spallation isotopes depends on the energy and composition spectrum of the radiation in the sample. The correlation found between He^3/Ne^{21} and Ne^{22}/Ne^{21} suggests that mainly variations in the neon production rate are the source for the observed variations in the He^3/Ne^{21} ratio. From tritium measurements it is known that the He^3 production rate in most chondrites is indeed constant within ±20% [40, 41]. The cross section for Ne^{21} production from Mg, Al and Si is roughly constant for protons with energies between 0.6 and 24 GeV, whereas the He^3 production cross section seems to be somewhat more energy dependent [9, 42]. Charged particles with energies below a few hundred MeV contribute relatively little to the production of

[38] H. HINTENBERGER, H. KÖNIG, L. SCHULTZ, H. WÄNKE, and F. WLOTZKA, Z. Naturforschg. **19 a**, 88 [1964].

[39] H. CRAIG, in Isotopic and Cosmic Chemistry, dedicated to H. C. UREY (ed. H. CRAIG, S. MILLER, and G. WASSERBURG), North-Holland Publ. Co., Amsterdam 1964.

[40] J. GEISS, H. OESCHGER, and P. SIGNER, Z. Naturforschg. **15 a**, 1116 [1960].

[41] K. GOEBEL and P. SCHMIDLIN, Z. Naturforschg. **15 a**, 79 [1960].

[42] K. GOEBEL, H. SCHULTES, and J. ZÄHRINGER, CERN-report CERN 64-12 [1964].

spallation isotopes. Secondary neutrons in this energy range will, however, make an appreciable contribution to the total production, because they are not slowed down by ionization. After cosmic radiation has passed through one interaction length, the number of neutrons should be equal to or larger than the number of protons. Neutrons with energies between ten and a few hundred MeV will, to a large extent, induce spallation reactions resulting in small ΔA, such as

$$Mg^{24}(n,2pn)Ne^{22}, \quad Mg^{24}(n,p2n)Na^{22}(\beta)Ne^{22},$$
$$Mg^{24}(n,\alpha)Ne^{21}.$$

Thus, in large stone meteorites secondary neutrons will make an appreciable contribution to the total neon production [33].

If this explanation holds, high He^3/Ne^{21} ratios should be found only in small meteorites. A comparison of Tables 1 and 6 and a survey of the literature shows that all meteorites with $Ne^{22}/Ne^{21} > 1.15$ are small, the recovered weights corresponding to radii of less than 15 cm.

The He^3/Ne^{21} production ratio in chondrites of the primary cosmic radiation must thus be equal to or higher than 7, the highest value observed. Such a ratio corresponds to an average energy of 600 MeV (cf. Fig. 4 in KIRSTEN, KRANKOWSKY, and ZÄHRINGER [9]).

In chondrites, Ar^{38} is produced in approximately equal amounts from calcium and iron. The production of Ar^{38} from Ca^{40} is similar to the production of Ne^{22} from Mg^{24}, i. e. mass loss $\Delta A = 2$ and heavy contribution by secondary neutrons in both cases. Therefore, it is to be expected that the Ne^{22}/Ar^{38} ratio is more constant than the He^3/Ar^{38} ratio. A comparison of meteorites with extreme He^3/Ne^{21} values shows that this is indeed true. The L-chondrites Walters, Bruderheim, and Maziba have constant Ne^{22}/Ar^{38} ratios of 7.8, 7.6 and 7.6, whereas the He^3/Ar^{38} ratios are 26, 36 and 47. The LL-chondrites Dhurmsala and Finney have Ne^{22}/Ar^{38} ratios of 9.0 and 8.7 and He^3/Ar^{38} ratios of 29 and 55. The average Ne^{22}/Ar^{38} ratios of H-, L- and LL-chondrites are 7.6, 8.2 and 8.7 respectively. The variations are, of course, due to the systematic differences in the iron contents of the three classes.

6.1.3. Diffusion Loss

Partial diffusion loss will mainly affect He^3/Ne^{21}. No great change is to be expected in the Ne^{22}/Ne^{21} ratio (preferential diffusion loss in certain minerals may result in small changes). Thus, diffusion loss will move a meteorite in the $He^3/Ne^{21} - Ne^{22}/Ne^{21}$ diagram parallel or nearly parallel to the ordinate in the direction of smaller He^3/Ne^{21} values.

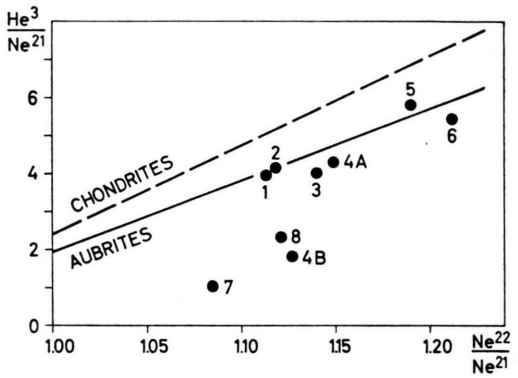

Fig. 4. $(He^3/Ne^{21})_{spall}$ versus $(Ne^{22}/Ne^{21})_{spall}$ correlation diagram for aubrites. The aubritic correlation line is not fitted but has been calculated from the one for chondrites. (1) Norton County, (2) Khor Temiki, (3) Bustee, (4A) and (4B) two Bishopville samples, (5) Shallowater, (6) Peña Blanca Spring, (7) Cumberland Falls, (8) Aubres.

As an illustration, we will discuss the case of the enstatite achondrites (aubrites). Figure 4 is a $He^3/Ne^{21} - Ne^{22}/Ne^{21}$ diagram for the aubrites. The data used are from EBERHARDT, EUGSTER, and GEISS [43] and KIRSTEN, KRANKOWSKY, and ZÄHRINGER [9]. The Ne^{22}/Ne^{21} ratios of the latter authors have been recalculated for $Ne^{20}/Ne^{22} = 9.80$ in the terrestrial atmosphere. The He^3 production rate in aubrites is 1.11 and the Ne^{21} production rate is 1.38 times higher than in chondrites [43]. For the same irradiation spectrum, He^3/Ne^{21} ratios are thus 20% smaller in aubrites than in chondrites. The Ne^{22}/Ne^{21} ratio is not affected because the Mg/Si ratios in aubrites and chondrites are virtually equal. The correlation line for aubrites, shown in Fig. 4, has been calculated from the correlation line for chondrites with

$$C(\text{aubrites}) = \tfrac{1.11}{1.38} \times C(\text{chondrites}),$$
$$m(\text{aubrites}) = \tfrac{1.11}{1.38} \times m(\text{chondrites}).$$

Six aubrites (Shallowater, one sample of Bishopville, Norton County, Khor Temiki, Bustee, Peña Blanca Spring) lie

[43] P. EBERHARDT, O. EUGSTER, and J. GEISS, J. Geophys. Res. **70**, 4427 [1965].

within $\pm 12\%$ of the correlation line. Cumberland Falls, Aubres and a second sample of Bishopville, however, have much lower He^3/Ne^{21} ratios than would correspond to their Ne^{22}/Ne^{21} values. These three meteorites must have suffered considerable He^3 diffusion losses. The difference in the Ne^{21} content of the two Bishopville samples is only 10%, whereas the He^3 differs by more than a factor of two. The Ne^{22}/Ne^{21} ratio in both Bishopville samples is the same within the limits of experimental error. From the Ne^{22}/Ne^{21} ratios, we deduce that the He^3/Ne^{21} production ratio was 3.5 in Cumberland Falls and 4.0 in Aubres.

From the foregoing discussion it is evident that the He^3/Ne^{21} ratio alone is not necessarily a good criterion for diffusion losses. It has recently been claimed [37] that the He^3/Ne^{21} ratio of 3.0 in the chondrite Weldona is due to strong diffusion loss. However, ZÄHRINGER [26] reports $Ne^{22}/Ne^{21} = 1.04$ and thus this meteorite lies close to the correlation line in Fig. 3.

6.2 Radiation Ages

The radiation age T_R of a meteorite is defined as

$$T_R = C^I/P_0^I \qquad (2)$$

where C^I is the concentration of a stable spallation isotope and P_0^I its production rate just prior to the fall of the meteorite. P_0^I can be inferred from the concentration of a suitable radioactive spallation isotope, such as H^3. Several different possible irradiation histories for stone meteorites have been proposed and discussed (cf. EBERHARDT, EUGSTER, and GEISS [43]). The most simple and basic one assumes that the meteorite was completely shielded from cosmic radiation until it was broken out of a larger body and exposed. If the production rate was constant during the whole exposure time, then the radiation age T_R dates this event.

Measurements of tritium in a number of chondrites have shown that the production rate of He^3 is the same in chondrites within approximately $\pm 20\%$ (l. c. [40, 41]). Thus, it is possible to calculate radiation ages of chondrites from He^3 concentrations alone, using an average production rate of 2×10^{-8} cc STP He^3/m.y. The error introduced by this assumption should be less than $\pm 20\%$.

Several authors have also derived radiation ages from Ne^{21} concentrations. However, the neon production rate is less constant than that of He^3 (see 6.1). Radiation ages calculated from Ne^{21} concentrations alone are therefore liable to have large errors. The same holds for radiation ages calculated from Ar^{38}.

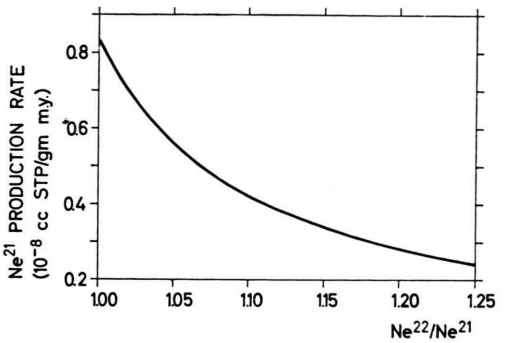

Fig. 5. Ne^{21} spallation production rate as function of $(Ne^{22}/Ne^{21})_{spall}$ ratio. A constant He^3 production rate of 2×10^{-8} cc STP/gm m. y. was assumed.

The correlation discovered between the He^3/Ne^{21} and Ne^{22}/Ne^{21} ratios can now be used for deriving Ne^{21} production rates. In Fig. 5 the Ne^{21} production rate is given as function of the Ne^{22}/Ne^{21}ratio. It has been calculated from Eq. (1), assuming constant He^3 production rate. In this way radiation ages can also be obtained from Ne^{21} concentrations, provided the Ne^{22}/Ne^{21} ratio has been measured with sufficient accuracy.

The radiation ages of the investigated meteorites are given in Table 6. They were calculated by assuming a constant He^3 production rate of 2×10^{-8} cc STP He^3/m.y. The ages obtained are in agreement with the salient features found for the radiation age distributions of the different chondrite classes (GEISS, OESCHGER, and SIGNER [40]); EBERHARDT and GEISS [8]; ANDERS [25]; ZÄHRINGER [26]). A detailed discussion seems therefore unnecessary.

7. Trapped Gases

In the course of this work we have found several new chondrites with large amounts of trapped gases (primordial gases). These are Tysnes Island and Dimmitt, containing "solar type" trapped gases; Mezö-Madaras, Tieschitz and Marion with "planetary type" trapped gases. Also Pseudo-Pultusk is a gas-rich meteorite, in accordance with He and Ne measurements on Pultusk [35]. The rare gas concentrations and isotopic composition in the trapped gas component of these and other meteorites will be discussed elsewhere.

Acknowledgements

The authors are greatly indebted to their collegues who supplied and prepared the meteorite samples used in this investigation: Prof. W. SCHOLLER, Naturhistorisches Museum, Wien; Dr. E. P. HENDERSON, U.S. National Museum, Washington; Prof. C. B. MOORE, Arizona State University, Tempe; Prof. J. ARNOLD, University of California, San Diego; Dr. G. KURAT, Naturhistorisches Museum, Wien; Prof. M. GRÜNENFELDER, ETH, Zürich; Prof. A. DE CASTELLO BRANCO, Serviços Geologicos, Lisboa; Prof. A. TUCEK, Narodni Museum, Praha; Prof. R. E. FOLINSBEE, University of Alberta, Edmonton; Proffs. R. DAVIES and O. SCHAEFFER, BNL, Brookhaven.

We are indebted to Dr. N. GRÖGLER for advice and help in the preparation of the meteorite samples. Our work has benefitted from stimulating discussions with Proffs. E. ANDERS, N. GRÖGLER, and F. G. HOUTERMANS.

We would like to thank Messrs. E. LENGGENHAGER, H. WYNIGER, H. HOFSTETTER, and R. LINIGER for their careful work in constructing the mass spectrometers; Miss A. STROTZ and Messrs. R. GASSER and T. REBER for their assistance in preparing and analyzing the samples; and Miss B. RAMSEIER for the preparation of the manuscript.

This work was supported by the Swiss National Science Foundation grants KAW/A 214, NF 2648, NF 3045, and NF 3468.

Kraftkonstantenberechnung nach einer Methode der nächsten Lösung

A. FADINI *

Lehrstuhl für Technische Mechanik (Prof. SLIBAR) der Technischen Hochschule, Stuttgart

(Z. Naturforschg. **21 a**, 426—430 [1966]; eingegangen am 30. November 1965)

Die Berechnung von Molekülkraftkonstanten aus der Säkulargleichung $|\mathbf{G}\cdot\mathbf{F}-\lambda\mathbf{E}|=0$ führt im allgemeinen auf eine unendliche reelle Lösungsmannigfaltigkeit **F**, wenn nur die inverse Matrix **G** der kinetischen Energie und die Spektralmatrix $\mathbf{L}=\mathrm{Diag}(\lambda_i)$ mit $i=1, 2, \ldots, n$ bekannt sind. Bei einer Reihe von Molekülen können Näherungslösungen $\mathbf{F}_{\text{näh}}$ bestimmt werden, und wir geben ein Verfahren an, durch das aus **F** eine Matrix $\mathbf{F}_{\min}$ als Kraftkonstantenmatrix ausgewählt wird, die der Näherungslösung $\mathbf{F}_{\text{näh}}$ am nächsten liegt. Für dieses sogen. erweiterte inverse Eigenwertproblem der Ordnung $n=2$ wird die Bedingung für die Existenz eines reellen Lösungsbereiches angegeben, die Lösungsmethode als Näherungsverfahren explizit dargestellt und das mathematische Modell der nächsten Lösung geometrisch interpretiert. An den beiden Molekülen BrCN und OCS wird das Verfahren erprobt. Im Falle gleicher Eigenwerte existiert für $n=2$ nur die eine reelle Lösung $\mathbf{F}(\lambda)=\lambda\cdot\mathbf{G}^{-1}$.

1. Die Berechnung von Molekülkraftkonstanten als „ein erweitertes inverses Eigenwertproblem“ [1]

Die klassische Theorie der Molekülkraftkonstanten führt auf die Berechnung der Kraftkonstantenmatrix **F** aus der Säkulargleichung

$$\det(\mathbf{G}\cdot\mathbf{F}-\lambda\mathbf{E})=0\,. \tag{1}$$

Dabei wird die Matrix **G** aus den Gleichgewichtsabständen, den Valenzwinkeln und Atommassen in gegebener Anordnung berechnet. Die Spektralmatrix $\mathbf{L}=\mathrm{Diag}(\lambda_i)$ mit $i=1, 2, \ldots, n$ ergibt sich aus den n Schwingungsfrequenzen des Moleküls, die dem RAMAN- oder den Ultrarotspektren entnommen werden.

Für $\mathbf{F}=\mathbf{F}_{\text{diag}}$ existieren $n!$ reelle und komplexe Lösungen [2]. Bei der Kraftkonstantenrechnung ist jedoch **F** mit

$$\mathbf{F}=\mathbf{F}_{\text{sym}}=(f_{ik})=(f_{ki}) \text{ mit } i, k=1, 2, \ldots, n \tag{2}$$

gesucht und dies führt im allgemeinen auf eine unendliche Lösungsmannigfaltigkeit für **F**. Wegen der Realität der Kraftkonstanten setzen wir die Existenz einer reellen Lösungsmannigfaltigkeit für **F** voraus.

Für eine Reihe von Molekülen ist es durch Hinzunahme zusätzlicher Daten möglich, physikalisch hinreichend genaue Näherungslösungen

$$\mathbf{F}_0=\mathbf{F}_{\text{sym},0}=\mathbf{F}_{\text{näh}} \tag{3}$$

anzugeben (siehe Abschnitt 3). Die beiden physikalischen Aussagen (1) und (3) werden sinnvoll

* Privatanschrift: 74 Tübingen, Breuningstr. 31.

[1] Das hier dargestellte Eigenwertproblem wurde bereits auf der GAMM-Tagung in Wien im April 1965 vorgetragen und das Lösungsverfahren „Quadratsummen-Minimum-Verfahren“ genannt [14]. Die geometrische Interpretation wurde auf dem 8. Europäischen Kongreß für Spektroskopie in Kopenhagen vom 14.—20. August 1965 vorgebracht [15].

[2] J. UHLIG, Z. Angew. Math. Mech. **38**, 284 [1958].